Universal Short-Circuit and Open-Circuit Fault Detection for an Inverter

B. Brown[1] and Z. Zhang[1]
[1] Clemson University, USA

***Abstract*—Short-circuit and open-circuit faults of a power device in an inverter often lead to catastrophic failure of the entire system if not detected and acted upon within a few microseconds. While a significant amount of research has been done on the fast and accurate protection and detection of short-circuit faults, there has been less success corresponding to open-circuit faults. Common downfalls include protection and detection that is application specific, takes longer than a couple of microseconds, and is not cost-effective. This paper proposes a new open-circuit fault protection and detection system integrated with a pre-existing desaturation protection short-circuit fault detection circuit. First, the operation principle of the newly proposed scheme is discussed. Second, the design consideration for such a scheme is detailed. Third, the scheme is verified through simulation under a case study. Results show the effectiveness and reliability of the proposed solution.**

***Index Terms*—Desaturation protection, open-circuit fault protection, reverse current faults.**

I. Introduction

The growth of electrical energy production throughout the past few decades is unmatched. In 2011, 40% of the energy consumed in the United States was electrical [1]. As this rise in electrical energy production increases, the demand for reliable, high-quality electrical components used in electrical energy production and conversion increases. While the reliability of electrical components used in electrical energy production has improved vastly over the past decades, the reliability of electrical components used in electrical energy conversion has lacked such drastic improvement.

In 2005, 30% of electricity flowed through power electronic converters [2]. This fact is no surprise considering power electronic converters are used in applications such as uninterruptable power supply systems, power supplies for telecommunication equipment, high voltage DC (HVDC) systems, distributed energy sources for renewable energy generation, battery energy storage systems, and power conversion systems for process technology [3]. Furthermore, 80% of electricity is expected to flow through power electronic converters in 2030 by the United States Department of Energy (DOE) as the nation pushes toward ambitious renewable energy penetration. However, these power electronic converters, specifically inverters, are often the bottleneck for reliable performance [4]. For example, based on the field data given by [5], photovoltaic (PV) inverters are responsible for 45% to 70% of PV service tickets, which significantly worsens the levelized cost of energy (LCOE) in the PV system. These inverters often fail due to the sensitive switching components within the inverter, such as Silicon Carbide (SiC) MOSFETs or Gallium Nitride (GaN) HEMTs, being damaged and producing a fault, even leading to cascaded catastrophic failure of the entire inverter. In order to prevent such calamity, fault protection and detection in inverters is needed.

There have been many previous efforts to solve the problem of fault protection and detection in inverters. The two most common faults that occur are short-circuit faults and open-circuit faults. Short-circuit faults result in abnormally large currents. As these currents increase, the components' temperatures within the inverter increase, leading to inverter failure. This permanent damage occurs on a sub-microsecond scale, especially for emerging wide bandgap (WGB) power semiconductors. Due to such an apparent problem, short-circuit faults within inverters have been extensively studied. One solution, called desaturation protection, is widely applied and documented in [6].

Open-circuit faults also have drastic effects on components within an inverter. Most power electronic loads are inductive, so when an open circuit occurs, and there is no place for the current through the load to flow, there is a massive voltage spike across the opened power device due to high di/dt. The components within the inverter cannot withstand such high voltages for extended periods, so the inverter is damaged.

As with the short-circuit fault, there have been many attempts at protecting against and detecting open-circuit faults. However, unlike with the short-circuit fault, there lacks a universal, fast, and cost-efficient open-circuit fault protection and detection system.

In [7] and [8], an open-circuit fault protection and detection scheme for grid-connected inverters is proposed. However, [7] focuses on detection in a wind energy conversion topology, and [8] focuses on detection in a grid-connected, three-phase, neutral point clamped topology. While both techniques successfully protect against and detect open-circuit faults within their given topologies, they are quite different. There is a trend of application-specific solutions throughout the related literature. As further examples, [9] considers a cascaded H-bridge multilevel inverter topology; [10] considers a T-type multilevel converter topology; and [11] considers a power converter in a PM-BLDC motor contained in an electric vehicle. Each solution proposed in [7]-[11] is significantly different due to its application-specific

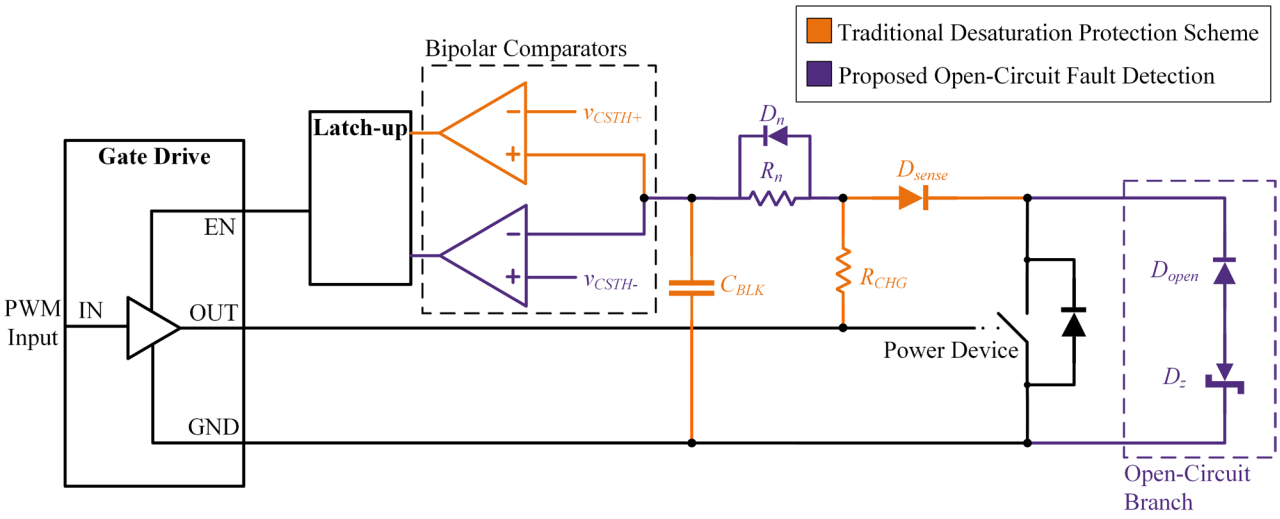

Fig. 1. Generic power device with protection and detection circuit and gate drive.

nature.

In recent literature, the speed and cost of protection and detection are two other significant issues pertaining to protecting against and detecting open-circuit faults in inverters. While [12] offers a solution for open-circuit fault protection and detection, it requires a minimum of 3.5 ms before protection and detection can occur. Newer data-driven and model-data-hybrid driven methods—[13] and [14] respectively—take a minimum of several switching periods (over 100 µs) before they protect against and detect open-circuit faults. Additionally, some solutions require multiple sensors, bringing with them a high cost, as seen in [7], [8], and [12].

Therefore, it is essential to make a new fault protection and detection design for power devices capable of detecting short-circuit and open-circuit faults within a few microseconds. The new design should be universal and inexpensive. Through the modification of pre-existing desaturation protection techniques, the proposed fault protection and detection system is shown in Fig. 1.

II. Design Methodology

In this section, the design illustrated in Fig. 1 is detailed. First, the short-circuit protection and detection the circuitry provides is highlighted, and then the novel open-circuit protection and detection the circuitry provides is described. At the end of the section, practical design considerations are given.

A. Desaturation Protection Design

A standard desaturation protection circuit is the foundation of the circuit shown in Fig. 1. This desaturation protection circuit (often called "desat") is used to protect against short-circuit faults and consists of the following: a charging resistor, R_{CHG}; a sensing diode, D_{sense}; a blanking capacitor, C_{BLK}; a positive comparator with a positive threshold voltage, v_{CSTH+}; and a latch-up circuit. The way in which the desaturation protection circuit functions is detailed in [6]. In order to leverage this circuit, the components contained within it are sized as desired.

The equation used for determining the positive threshold voltage is given as

$$v_{CSTH+} = v_{DSTH} + v_{f\_Dsense} \tag{1}$$

where v_{DSTH} is the drain-to-source threshold voltage of the power device, and v_{f_Dsense} is the forward voltage of the sensing diode, D_{sense}. The drain-to-source threshold voltage is found by examining the datasheet of the power device used in the circuit. For a given gate-to-source voltage, v_{GS}, and threshold drain current, i_{DTH}, there is a corresponding v_{DSTH}. The forward voltage of the sensing diode is found from the sensing diode's datasheet.

Following the calculation for the positive threshold voltage, the blanking capacitance is found using

$$C_{BLK} > k_{Cj\_Dsense} \cdot C_{j\_Dsense} \tag{2}$$

where C_{j_Dsense} is the junction capacitance of the sensing diode, and k_{Cj_Dsense} is a scaling factor relating the junction capacitance of the sensing diode and the blanking capacitance. The junction capacitance of the sensing diode is found from the sensing diode's datasheet. The scaling factor, k_{Cj_Dsense}, is designed to ensure that C_{BLK} is significantly larger than C_{j_Dsense} to avoid the noise current induced by $C_{j\_Dsense} \cdot dv_{DS}/dt$. Practically, it is chosen to be at least 50.

Next, the charging resistance is calculated. However, in order to calculate the charging resistance, the time constant of the circuit is first chosen according to the desired blanking time. Generally, it is chosen to be much less than one switching period. This time constant is represented as

$$\tau = R_{CHG} \cdot C_{BLK} \tag{3}$$

Rearranging (3) to solve for R_{CHG} yields

$$R_{CHG} = \frac{\tau}{C_{BLK}} \tag{4}$$

The final aspect of the desaturation protection design is a latch-up circuit. Internally, this circuit consists of a simple SR latch with the reset pin low. Therefore, when a fault is detected, the output of the latch-up circuit reports it regardless of future inputs. This output signal is tied to the gate drive. Internally, this gate drive turns off the power device when a fault signal is received. In addition, a "soft" resistor connected to the gate of the transistor is activated, increasing the gate resistance and allowing for a "soft" turn-off. Therefore, through desaturation protection, a short-circuit fault is detected, and the gate drive of the transistor switching device is shut down, preventing cascaded failure throughout the system.

B. Additional Open-Circuit Fault Protection

There are two different classifications of inverter open-circuit faults, and it is essential to understand the difference between them. An open-circuit fault can occur when current is flowing through the power device in the forward direction, from drain to source (using MOSFETs' terminology as an example), or when current is flowing through the power device in the reverse direction, either from source to drain or through the freewheeling diode [15]. The understanding of this phenomenon draws on the semiconductor physics of lateral-structure MOSFETs provided by [16] and [17]. After the different types of open-circuit faults are examined, the open-circuit fault protection and detection design is detailed.

If current flows through the power device in the forward direction, it flows from the drain to the source. If an open-circuit fault occurs when current flows through the power device in the forward direction, the current through the load flows through the freewheeling diode of the complimentary power device. Therefore, there is no voltage spike across the lower power device due to high *di/dt*, and catastrophic failure is avoided. However, having the power device open-circuited is still a control issue, and the inverter cannot function properly without repair. Hence, it is still important to be able to detect the open-circuit fault. While seemingly unknown, desaturation protection allows for the detection of open-circuit faults when current flows through the power device in the forward direction. When a forward current open-circuit fault occurs, the drain-to-source voltage of the power device becomes the DC bus voltage. Assuming this voltage is greater than the positive threshold voltage, v_{CSTH+}, of the desaturation protection, the open-circuit fault will be detected, and the power device will be turned off.

If current flows through the power device in the reverse direction, it flows from the source to the drain. Whereas forward current only flows through the channel of the power device, reverse current can flow through either the channel or the freewheeling diode of the power device. These reverse current open-circuit faults are estimated to account for about half of all power device open-circuit faults since current flows in the forward direction about the same amount of time it flows in the reverse direction in inverter circuitry. With only traditional desaturation protection implemented, it can take anywhere from 50 µs to 200 µs (depending on switching frequency) before reverse current open-circuit faults turn into forward current open-circuit faults and can subsequently be detected and protected. Since there is nowhere for reverse current to flow if an open-circuit fault occurs, this amount of elapsed time will likely allow permanent damage to the device and the surrounding inverter.

Nothing new must be developed to protect against and detect forward current open-circuit faults—desaturation protection is sufficient. However, to protect the inverter against reverse current open-circuit faults and detect when reverse current open-circuit faults occur, the standard desaturation protection circuit must be enhanced. These enhancements are illustrated in Fig. 1. They include three addendums to the traditional desaturation protection circuitry. The first addendum is the insertion of a branch in parallel with the drain and source terminals of the power device consisting of a diode, D_{open}, in anti-series with a Zener diode, D_z. The second addendum is the inclusion of a noise immunity resistor, R_n, and its corresponding bypass diode, D_n. The third addendum is the introduction of a bipolar comparator with a negative threshold voltage, v_{CSTH-}. The output of this comparator is connected to the same latch-up circuit used for short-circuit fault detection.

The addition of the branch consisting of a diode in anti-series with a Zener diode diminishes the catastrophic failure due to a reverse current open-circuit fault and allows for fault detection. During normal operation, current does not flow through this branch because of the existence of the Zener diode blocking the current. When a reverse current open-circuit fault occurs, the Zener diode enters its breakdown region, allowing current to flow through the branch. As a result, the voltage across the branch is clamped to a certain value and is expressed as

$$v_{OC} = -v_{f\_Dopen} - v_{z,b} \tag{5}$$

where v_{f_Dopen} is the forward voltage of the diode, and $v_{z,b}$ is the breakdown voltage of the Zener diode. The breakdown voltage of the Zener diode is up to the user to decide. Whereas traditionally there is no place for the current flowing through the load to go when a reverse current open-circuit fault occurs, it now has an alternative path.

The noise immunity resistor and corresponding bypass diode are essential to prevent the false triggering of the detection system due to switching ringing and interference [19]. They prevent the blanking capacitor from drastic fluctuations in the sensed voltage. Therefore, this noise immunity branch delays detection by approximately a microsecond, which is determined by the maximum switching time of the device under investigation. However, it is important to note that the protection given by the new open-circuit branch is ubiquitous.

Due to the constant voltage across the newly implemented open-circuit branch, it is easy to detect when a reverse current open-circuit fault occurs. The negative comparator leverages the voltage across the blanking capacitor and compares it with a negative threshold voltage given by

$$v_{CSTH-} = -(v_{f\_Dopen} + v_{z,b})x \tag{6}$$

where x is a scaling factor between 80-100% to compensate for potential nonidealities and ensure detection of the open-circuit fault. The outputs of the negative comparator and positive comparator are tied together before the latch-up circuit. This is done practically through an OR gate. Therefore, regardless of which fault occurs, the output of the latch-up circuit indicates if a fault has occurred.

C. Design Considerations

Aside from the previous theory used to size the components shown in Fig. 1, there are still a few considerations that need to be made before the circuit can be implemented in reality. In particular, special design considerations need to be made for five key components: the charging resistor, the sensing diode, the blanking capacitor, the Zener diode, and the standard diode contained in the open-circuit branch.

The first component that needs to be reconsidered is the charging resistor, R_{CHG}. Like always, the resistor's power rating corresponds to the power dissipated in the resistor. The power dissipated in the charging resistor is

$$P_R = \frac{{v_R}^2}{R_{CHG}} \tag{7}$$

where

$$v_R = v_{GS} - (v_{DS} + v_{f\_Dsense}) \tag{8}$$

Under a traditional desaturation protection scheme, v_R is always less than v_{GS} since both v_{DS} and v_{f_Dsense} are positive values. However, with the additional open-circuit fault detection functionality, v_{DS} is negative when an open-circuit fault occurs. As a result, it is now possible for v_R to be greater than v_{GS}, and therefore, special attention must be given when determining the power rating of the charging resistor. It is also important to note that (7) and (8) are only applicable when considering the power device when it is turned on, undergoing a switching commutation, or experiencing a fault, since the power dissipated in the resistor when the power device is turned off is approximately zero.

The second component that needs to be reconsidered is the sensing diode, D_{sense}. When the diode is not blocking the drain-to-source voltage, the current through the sensing diode is

$$i_{Dsense} = \frac{v_{GS} - v_{f\_Dsense} - v_{DS}}{R_{CHG}} \tag{9}$$

As with the resistor, when an open-circuit fault occurs, v_{DS} is negative, and i_{Dsense} is greater than it is under standard desaturation protection. As a result, special attention must be given to the maximum current flowing through the diode. In addition, the breakdown voltage of the sensing diode must be greater than the possible off-state voltage of the power device. Furthermore, it is crucial that the sensing diode is a super-fast recovery diode or a Schottky diode to reduce the noise produced when the sensing diode turns off. Likewise, the junction capacitance of the sensing diode should be as small as possible in order to reduce the amount of displacement current induced during *dv/dt* when the power device turns off [6].

The third component that needs to be reconsidered is the blanking capacitor, C_{BLK}. As shown previously, the blanking capacitance is sized according to (2) and (3). The blanking capacitor should also be able to handle a voltage of

$$v_C = v_{DS} - v_{Dsense} \tag{10}$$

Special attention should be given during switching transitions due to possible overshoot in voltages.

The fourth component that must be considered is the Zener diode contained in the open-circuit branch, D_z. When a reverse current open-circuit fault occurs, the current through the load flows through the open-circuit branch, meaning the load current flows through the Zener diode. Therefore, the Zener diode must be able to handle a pulse current equal to the rated current of the load. In addition to the current flowing through the load, the Zener diode must absorb the energy stored in the load. If the load is inductive, the Zener diode must be able to handle an energy of

$$E_Z = \frac{1}{2} L \cdot (I_{max})^2 \tag{11}$$

where L is the inductance of the load and I_{max} is the maximum instantaneous current flowing through the load.

The fifth component that needs to be considered is the standard diode contained in the open-circuit branch, D_{open}. This diode must be sized to handle the voltage of the power device when it is turned off. Like the Zener diode, the diode in the open-circuit branch must be able to handle a pulse current equal to the rated current of the load.

III. Simulation Verification

The reverse current open-circuit fault protection and detection scheme has been outlined and detailed. Before building it in an experimental setup, however, it is important to demonstrate its effectiveness in a simulation. Hence, this section focuses on the simulation verification of the new protection and detection circuitry.

Given a desired reverse current open-circuit fault detection speed, each component of the new scheme can be determined using (1)-(11). Afterward, the novel circuit architecture shown in Fig. 1 can be added to any power device gate drive.

Showcasing the effectiveness of the reverse current open-circuit fault protection and detection scheme in every inverter topology is not feasible. Therefore, a case study utilizing the new circuitry is conducted. Two SiC MOSFETs are placed in a single-phase inverter topology. A reverse current open-circuit detection speed of ~2.5 µs is targeted. The DC bus voltage of the circuit is 800 V, and

TABLE I
SIMULATION PARAMETERS

Parameter	Value
R_{CHG}	240 Ω
C_{BLK}	6 nF
R_n	240 Ω
v_{CSTH+}	11.15 V
v_{CSTH-}	-8 V
$v_{z,b}$	10 V

an inductive load current of 20 A enters the middle node of the circuit. Using (1)-(11), the values of the various components in Fig. 1 are calculated. These values are listed in Table I, and the system is simulated using Synopsys/Saber with detailed device models. Stray resistance and inductance are added to account for the parasitic ones in practice. It is crucial to show that the new reverse current open-circuit fault protection and detection circuitry successfully protects against and detects short-circuit faults, forward current open-circuit faults, and reverse current open-circuit faults.

While there is a given topology with specific values for each component used in this case study, it is again important to note that the proposed solution is universal in its nature. This is due to its device-level protection and detection design.

A. Short-Circuit Fault

To illustrate the effects of short-circuit faults, the upper power device is turned off, while the lower power device is turned on. This configuration results in no drain current through the upper power device and 800 V dropped across the upper power device. The short-circuit fault is introduced by turning the upper power device on at 100 µs. The effects of such an action are shown in Fig. 2(a) and Fig. 2(b) by the dotted orange lines labeled "NP," which stands for no protection. Fig. 2(a) shows the drain current of the upper power device increase to above 200 A, even though the load has a rating of 20 A, causing increased drain-to-source voltage per power device I-V characteristics. This effect is shown in Fig. 2(b), where it is seen that the drain-to-source voltage of the device increases to about 200 V. With such a large drain current and drain-to-source voltage, the power dissipated in the upper power device is unsustainable, and permanent damage is likely to occur.

As stated before, short-circuit faults are protected through the desaturation protection scheme. While desaturation protection has previously been proven successful at detecting short-circuit faults, the proof is given here to show that the proposed integrated solution is also successful at detecting short-circuit faults.

The same fault that is used to create the "NP" signals of Fig. 2(a) and Fig. 2(b) is once again produced to create the "P" signals, which stands for protection, of Fig. 2(a)-(d). The only difference is that the newly proposed scheme shown in Fig. 1 is now implemented into the gate drive of the upper power device.

Before the fault occurs, the upper power device's drain current and drain-to-source voltage are equivalent to their corresponding "NP" signals. Since the upper power device is off at time zero, the voltage across the blanking capacitor

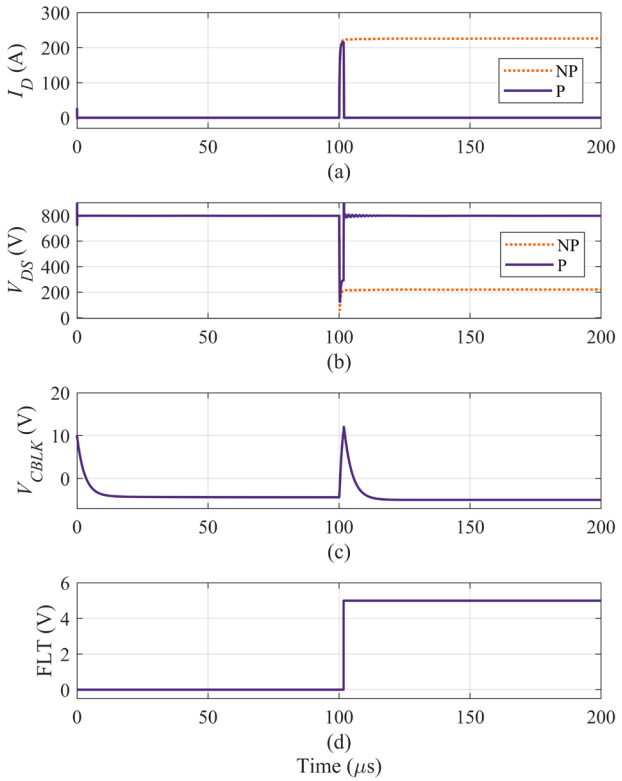

Fig. 2. Effect of short-circuit fault with and without new protection and detection scheme on (a) drain current, (b) drain-to-source voltage, (c) voltage across the blanking capacitor, and (d) fault signal.

charges to the gate-to-source voltage, which is -5 V. Since no fault has occurred, the fault signal is 0 V.

When the fault occurs at 100 µs, the drain current and drain-to-source voltage initially follow the same pattern as their corresponding "NP" signals. The drain current of the power device reaches just over 200 A in less than 1 µs. Since the upper power device is turned on, the voltage across the blanking capacitor begins to follow the drain-to-source voltage. After 1.736 µs, the voltage across the blanking capacitor reaches the positive threshold voltage of 11.15 V, and the fault flag is triggered. The upper power device is turned off at this instant, and the drain current quickly and smoothly falls to 0 A. Such a smooth transition when the gate is turned off does not occur for the drain-to-source voltage. A transient spike takes the drain-to-source voltage just over 1 kV. Following this transient, the drain-to-source voltage experiences some parasitic ringing and approaches its steady-state value of 800 V. Despite this transient behavior of the drain-to-source voltage, the voltage across the blanking capacitor remains smooth due to the noise immunity portion of the new circuitry. As evident by this test, the new protection and detection scheme successfully detects and protects against short-circuit faults, and in this case, does both in 1.736 µs.

B. Forward Current Open-Circuit Fault

To illustrate the effects of a forward current open-circuit fault, the upper power device is turned on while the lower power device is turned off. For this test only, the load of the system is placed across the lower power device, meaning the load current is flowing out of the middle node

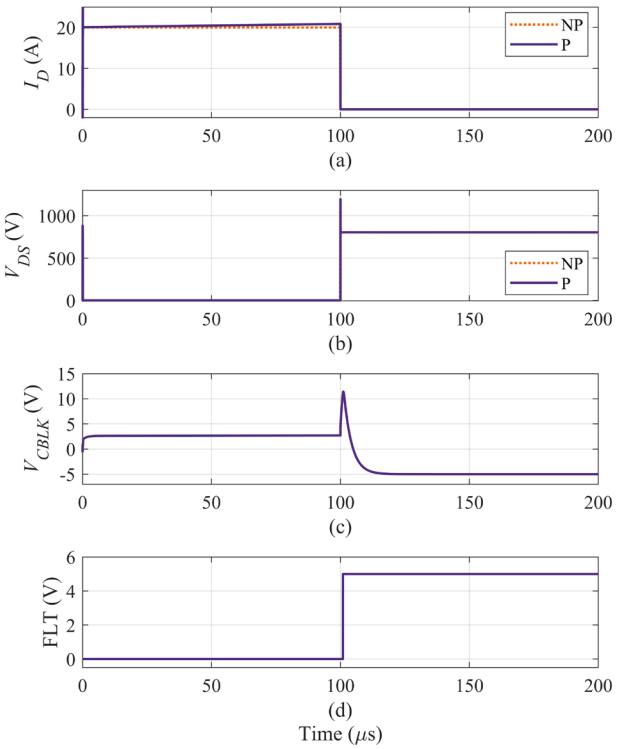

Fig. 3. Effect of forward current open-circuit fault with and without new protection and detection scheme on (a) drain current, (b) drain-to-source voltage, (c) voltage across the blanking capacitor, and (d) fault signal.

and from the drain to the source of the upper power device. At 100 µs, an open circuit is introduced in the upper power device, emulating a forward current open-circuit fault.

The results of this test without the new protection and detection scheme are shown by the "NP" signals in Fig. 3(a) and Fig. 3(b). Initially, the drain current is the same as the load current, and the drain-to-source voltage is approximately 0 V. When the fault occurs, the drain current of the upper power device decreases almost instantly to 0 A. However, the drain-to-source voltage of the upper power device spikes to around 1.2 kV and then steadies to the DC bus voltage of 800 V.

While the drain-to-source voltage increases during a forward current open-circuit fault, it is not nearly as detrimental to the system as a short-circuit fault or a reverse current open-circuit fault. This is because the load current flows through the freewheeling diode of the lower power device. However, a control issue arises since the gate of the upper power device is still turned on. This could be a significant problem if the current direction were to switch (like in inverter applications), and the forward current open-circuit fault turned into a reverse current open-circuit fault. Therefore, it is still essential to be able to detect such a fault. The protection scheme shown in Fig. 1 can perform forward current open-circuit fault detection.

Running the same test as before but including the new protection and detection scheme in the gate drive of the upper power device results in the "P" signals shown in Fig. 3(a)-(d). Before the fault occurs, it is seen that the initial drain current through the upper power device is approximately 20 A. There is a minute difference between the drain current of the "P" signal and the drain current of the "NP" signal. This difference is due to the load that is used in the simulation. For the "NP" signal, a current source with 20 A is used, whereas for the "P" signal, a non-ideal inductor with an initial current of 20 A is used. The non-ideal inductor is chosen for the test including the new protection and detection scheme to replicate a real-world environment more accurately. Despite this subtle difference, there should not be any difference in the capability of fault protection and detection. The initial drain-to-source voltage of the upper power device is 1-2 V because of a small amount of internal device resistance, and the initial voltage across the blanking capacitor is the sum of the drain-to-source voltage and the forward voltage of the sensing diode, which is around 2.5 V.

When the fault occurs at 100 µs, the drain current goes to 0 A as expected. Since the load current flows through the freewheeling diode of the lower power device, the drain-to-source voltage behaves just as it did without the protection and detection scheme in place; an initial spike in the drain-to-source voltage is observed due to the di/dt of the stray inductances in the circuit; in steady-state, the upper power device blocks the DC bus voltage of 800 V.

Since the upper power device is turned on, the voltage across the blanking capacitor begins to follow the drain-to-source voltage. After 0.955 µs, the voltage across the blanking capacitor reaches the positive threshold voltage of 11.15 V, and the fault flag is triggered. At this point, the upper power device is turned off, and the voltage across the blanking capacitor smoothly decreases to -5 V. As evident by this test, the new protection and detection scheme successfully detects and protects against forward current open-circuit faults, and in this case, does both in 0.955 µs.

Note that the time of fault detection in this case is less than the time of detection in the short-circuit case. This is because the distance between 11.15 V and 2.5 V is less than the difference between 11.15 V and -5 V, so the voltage across the blanking capacitor reaches the positive threshold voltage faster in a forward current open-circuit fault than it does in a short-circuit fault.

C. Reverse Current Open-Circuit Fault

As mentioned in Section II, reverse current open-circuit faults can occur when reverse current flows through the power device's freewheeling diode or when reverse current flows primarily through the inversion channel of the power device. If the power device is turned off, the reverse current flows through the power device's freewheeling diode. If the power device is turned on, the reverse current is primarily flowing through the inversion channel of the power device. To highlight the full capability of the new protection and detection scheme, its effectiveness under both types of reverse current open-circuit faults is considered.

1) Freewheeling Diode

To illustrate the effects of a reverse current open-circuit fault of the freewheeling diode, the upper power device is turned off, and the lower power device is turned off. As with the short-circuit test, the load is placed across the upper power device, and hence, the load current enters the middle node. Therefore, the load current is flowing

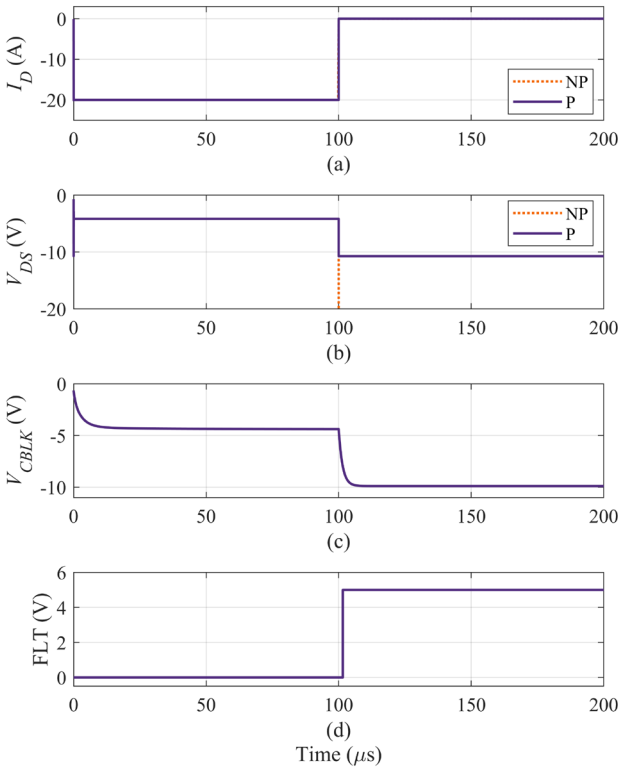

Fig. 4. Effect of reverse current open-circuit fault in freewheeling diode with and without new protection and detection scheme on (a) drain current, (b) drain-to-source voltage, (c) voltage across the blanking capacitor, and (d) fault signal.

through the freewheeling diode of the upper power device. At 100 µs, an open circuit is introduced in the upper power device, emulating a reverse current open-circuit fault.

The results of this test without the new protection and detection scheme are shown by the "NP" signals in Fig. 4(a) and Fig. 4(b). Initially, the drain current of the upper power device is -20 A, indicating the load current is flowing in the reverse direction through the power device (the freewheeling diode of the power device in this case). Furthermore, the drain-to-source voltage of the power device is around -4 V due to the voltage drop across the freewheeling diode. When the open-circuit fault occurs, the drain current of the upper power device decreases to zero as expected. The drain-to-source voltage of the power device plummets to drastically low numbers (around -10 MV in a matter of nanoseconds in this case study). Such high voltage will damage the system if maintained for any time.

The severity of this type of fault should not be understated. Combining the pre-existing desaturation protection, the open-circuit branch consisting of a diode and a Zener diode in anti-series, the noise immunity branch, and the negative voltage comparator allows this type of reverse current open-circuit fault to be protected and detected.

Running the same test as before but including the new protection and detection scheme in the gate drive of the upper power device results in the "P" signals shown in Fig. 4(a)-(d). Before the fault occurs, the drain current and drain-to-source voltage are identical to their corresponding "NP" signals. The initial voltage across the blanking capacitor smoothly reaches the drain-to-source voltage value, around -4 V.

When the fault occurs at 100 µs, the drain current goes to 0 A as expected. However, the drain-to-source voltage is clamped to the breakdown voltage of the Zener diode plus the forward voltage of the anti-series diode within 10 ns. Therefore, the drain-to-source voltage is clamped to around -10 V. As a result, the reverse current open-circuit fault is protected almost instantaneously. The voltage across the blanking capacitor follows a very similar trend to the drain-to-source voltage and smoothly approaches -10 V, following the RC characteristics of the circuit. After 1.562 µs, the voltage across the blanking capacitor reaches the negative threshold voltage of -8 V, and the fault flag is triggered.

As evident by this test, the new protection and detection scheme successfully protects against and detects reverse current open-circuit faults of the freewheeling diode. The protection against reverse current open-circuit faults of the freewheeling diode is immediate, and in this case, the detection of reverse current open-circuit faults of the freewheeling diode occurs in 1.562 µs.

2) Power Device Channel

To illustrate the effects of a reverse current open-circuit fault of the inversion channel of the power device, the upper power device is turned on, and the lower power device is turned off. The load is placed across the upper power device; hence, the load current enters the middle node. Therefore, the load current is primarily flowing through the inversion channel of the upper power device. At 100 µs, an open circuit is introduced in the upper power device, emulating a reverse current open-circuit fault.

The results of this test without the new protection and detection scheme are shown by the "NP" signals in Fig. 5(a) and Fig. 5(b). Initially, the drain current of the upper power device is -20 A, indicating the load current is flowing in the reverse direction through the power device (primarily through the power device channel in this case). Furthermore, the drain-to-source voltage of the power device is around -1 V due to the small voltage drop across the device's channel. Note that this voltage is less than the voltage of the previous case when the current only flows through the freewheeling diode. When the open-circuit fault occurs, the drain current of the upper power device decreases to zero as expected. The drain-to-source voltage of the power device plummets to drastically low numbers (around -10 MV in a matter of nanoseconds in this case study). Such high voltage will damage the system if maintained for any time.

The severity of this type of fault is clearly on par with the severity of the reverse current open-circuit fault of the freewheeling diode. However, through the combination of the pre-existing desaturation protection, the open-circuit branch consisting of a diode and a Zener diode in anti-series, the noise immunity branch, and the negative voltage comparator, this type of reverse current open-circuit fault can be protected and detected.

Running the same test as before but including the new protection and detection scheme in the gate drive of the upper power device results in the "P" signals shown in Fig.

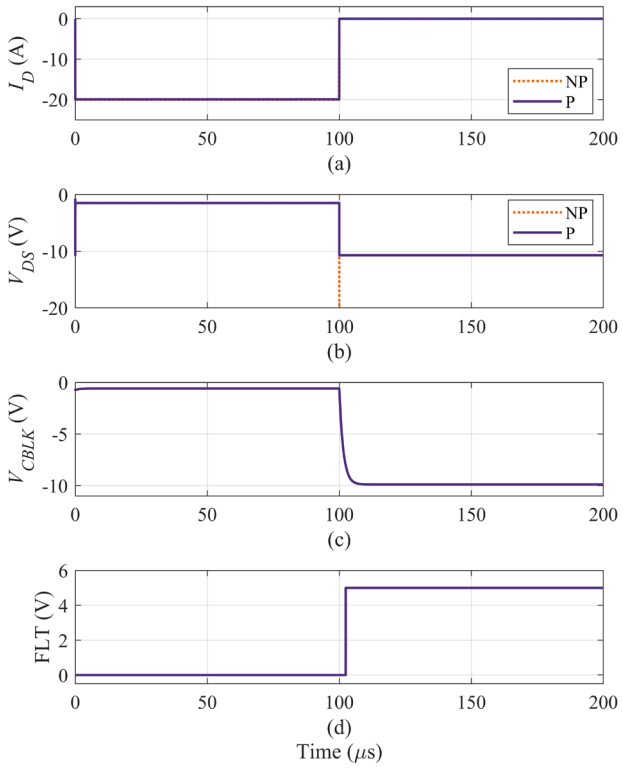

Fig. 5. Effect of reverse current open-circuit fault in power device channel with and without new protection and detection scheme on (a) drain current, (b) drain-to-source voltage, (c) voltage across the blanking capacitor, and (d) fault signal.

5(a)-(d). Before the fault occurs, the drain current and drain-to-source voltage are identical to their corresponding "NP" signals. The initial voltage across the blanking capacitor smoothly reaches the drain-to-source voltage value, around -1 V.

When the fault occurs at 100 µs, the drain current goes to 0 A as expected. However, the drain-to-source voltage is clamped to the breakdown voltage of the Zener diode plus the forward voltage of the anti-series diode within 10 ns. Therefore, the drain-to-source voltage is clamped to around -10 V. As a result, the reverse current open-circuit fault is protected almost instantaneously. The voltage across the blanking capacitor follows a very similar trend to the drain-to-source voltage and smoothly approaches -10 V, following the RC characteristics of the circuit. After 2.403 µs, the voltage across the blanking capacitor reaches the negative threshold voltage of -8 V, and the fault flag is triggered. While not shown in any waveform, the upper power device is consequently turned off to prevent any control issues from arising in the future.

As evident by this test, the new protection and detection scheme successfully protects against and detects reverse current open-circuit faults of the device channel. The protection against reverse current open-circuit faults of the device channel is immediate, and in this case, the detection of reverse current open-circuit faults of the device channel occurs in 2.403 µs.

Note that the time of fault detection in this case is more than the time of detection in the case of the freewheeling diode. This is because the distance between -1 V and -8 V is more than the difference between -4 V and -8 V, so the voltage across the blanking capacitor reaches the negative threshold voltage faster in a reverse current open-circuit fault of the freewheeling diode than it does in a reverse current open-circuit fault of the device channel.

IV. Conclusions

This paper proposes a new method for protecting against and detecting all common types of faults in inverter circuitry: short-circuit faults, forward current open-circuit faults, and reverse current open-circuit faults. This is done by enhancing pre-existing desaturation protection circuitry. The physics behind the need for the new protection and detection scheme is discussed, and practical design considerations necessary for the real-life implementation of the new scheme are given.

Simulation results show that the new protection and detection circuitry (1) protects against and detects short-circuit faults in as fast as 1.736 µs, depending on the size of the charging resistor and blanking capacitor; (2) protects against and detects forward current open-circuit faults in 0.955 µs, depending on the size of the charging resistor and blanking capacitor; and (3) protects against reverse current open-circuit faults within 10 ns, while detecting reverse current open-circuit faults of the freewheeling diode in 1.562 µs and detecting reverse current open-circuit faults of the power device channel in 2.403 µs, both times depending on the size of the noise immunity resistor, charging resistor, and blanking capacitor.

In addition to the fast protection and detection speeds the new scheme produces, it is also cost-efficient due to a complete lack of sensors—only cheaper, easier to obtain components are required. Further, it is universal due to its power device level implementation. Theoretically, it can be embedded in any inverter circuitry. In the future, various types of power devices and topologies can be experimentally tested to demonstrate the universal nature of the newly proposed fault protection and detection scheme.

References

[1] U.S. Energy Information Administration, "Annual Energy Review 2011." U.S. Department of Energy, Washington, DC, Sep-2012.

[2] Power America, "About Wide Bandgap Semiconductors," Power America Institute, Jan-2018. [Online]. Available: https://poweramericainstitute.org/about-poweramerica/lets-learn-about-power-electroncis/. [Accessed: Jul-2021].

[3] C. Wan, M. Huang, C. K. Tse and X. Ruan, "Effects of Interaction of Power Converters Coupled via Power Grid: A Design-Oriented Study," in IEEE Transactions on Power Electronics, vol. 30, no. 7, pp. 3589-3600, July 2015, doi: 10.1109/TPEL.2014.2349936.

[4] C. Wan, M. Huang, C. K. Tse, S. -C. Wong and X. Ruan, "Nonlinear Behavior and Instability in a Three-Phase Boost Rectifier Connected to a Nonideal Power Grid With an Interacting Load," in IEEE Transactions on Power Electronics, vol. 28, no. 7, pp. 3255-3265, July 2013, doi: 10.1109/TPEL.2012.2227505.

[5] P. Hacke, S. Lokanath, P. Williams, A. Vasan, P. Sochor, G. Mani, H. Shinohara and S. Kurtz, "A status review of photovoltaic power conversion equipment reliability, safety, and quality assurance protocols," Renewable and

Sustainable Energy Reviews, vol. 82, pp. 1097-1112, Feb. 2018, doi: 10.1016/j.rser.2017.07.043.
[6] F. Wang and Z. Zhang, "Protection design for double pulse test," in Characterization of Wide Bandgap Power Semiconductor Devices, Vol. 128, IET Energy Engineering Series, London: Institution of Energy and Technology, 2018, pp. 141-163.
[7] T. Kamel, Y. Biletskiy and L. Chang, "Fault Diagnoses for Industrial Grid-Connected Converters in the Power Distribution Systems," in IEEE Transactions on Industrial Electronics, vol. 62, no. 10, pp. 6496-6507, Oct. 2015, doi: 10.1109/TIE.2015.2420627.
[8] U. Choi, J. Lee, F. Blaabjerg and K. Lee, "Open-Circuit Fault Diagnosis and Fault-Tolerant Control for a Grid-Connected NPC Inverter," in IEEE Transactions on Power Electronics, vol. 31, no. 10, pp. 7234-7247, Oct. 2016, doi: 10.1109/TPEL.2015.2510224.
[9] A. Anand, N. Raj, S. George and Jagadanand G, "Open switch fault detection in Cascaded H-Bridge Multilevel Inverter using normalised mean voltages," 2016 IEEE 6th International Conference on Power Systems (ICPS), 2016, pp. 1-6, doi: 10.1109/ICPES.2016.7584128.
[10] J. He, N. A. O. Demerdash, N. Weise and R. Katebi, "A Fast On-Line Diagnostic Method for Open-Circuit Switch Faults in SiC-MOSFET-Based T-Type Multilevel Inverters," in IEEE Transactions on Industry Applications, vol. 53, no. 3, pp. 2948-2958, May-June 2017, doi: 10.1109/TIA.2016.2647720.
[11] G. Guruvareddiyar and B. Subathra, "An Open and Short Circuit Switch Fault of Power Converters in PM-BLDC Motor in Electric Vehicle," 2019 IEEE International Conference on Clean Energy and Energy Efficient Electronics Circuit for Sustainable Development (INCCES), 2019, pp. 1-3, doi: 10.1109/INCCES47820.2019.9167737.
[12] S. Yang, Y. Tang and P. Wang, "Seamless Fault-Tolerant Operation of a Modular Multilevel Converter With Switch Open-Circuit Fault Diagnosis in a Distributed Control Architecture," in IEEE Transactions on Power Electronics, vol. 33, no. 8, pp. 7058-7070, Aug. 2018, doi: 10.1109/TPEL.2017.2756849.
[13] Y. Xia, Y. Xu and B. Gou, "A Data-Driven Method for IGBT Open-Circuit Fault Diagnosis Based on Hybrid Ensemble Learning and Sliding-Window Classification," in IEEE Transactions on Industrial Informatics, vol. 16, no. 8, pp. 5223-5233, Aug. 2020, doi: 10.1109/TII.2019.2949344.
[14] Z. Li, Y. Gao, X. Zhang, B. Wang and H. Ma, "A Model-Data-Hybrid-Driven Diagnosis Method for Open-Switch Faults in Power Converters," in IEEE Transactions on Power Electronics, vol. 36, no. 5, pp. 4965-4970, May 2021, doi: 10.1109/TPEL.2020.3026176.
[15] R. W. Erickson, D. Maksimovic, Fundamentals of Power Electronics, Springer, 2001.
[16] J. P. Colinge, C. A. Colinge, Physics of Semiconductor Devices, Kluwer Academic Publishers, 2002.
[17] R. Anderson, B. Anderson, Fundamentals of Semiconductor Devices, McGraw Hill, 2004.
[18] B. Brown, "Failure Mode and Effects Analysis for a Photovoltaic Inverter," NERC Webinar, December 2022.
[19] X. Huang et al., "Comprehensive Analysis and Improvement Methods of Noise Immunity of Desat Protection for High Voltage SiC MOSFETs With High DV/DT," in IEEE Open Journal of Power Electronics, vol. 3, pp. 36-50, 2022, doi: 10.1109/OJPEL.2021.3134498.